JOURNAL OF ELECTROMAGNETIC ENGINEERING AND SCIENCE, VOL. 22, NO. 5, 571~575, SEP. 2022

https://doi.org/10.26866/jees.2022.5.r.124
ISSN 2671-7263 (Online) · ISSN 2671-7255 (Print)

Omega-K Algorithm Using Plane Wave Approximation for Forward-Looking Imaging Radar

Byunglae Cho · Sungwon Hong · Kichul Yoon*

Abstract

We propose an Omega-K algorithm that uses plane wave approximation for image formation in forward-looking imaging radar (FIRA) with the multi-input/double-output configuration. We assume that each of the transmitting antennas is located at the center of the receiving antenna array by applying a virtual antenna array. Then, we solve numerical equations in an approximation of the plane wave with the direction normal to the antenna array. Finally, we can obtain an image by proceeding with the following steps in order: the matched filtering, Stolt interpolation, two-dimensional inverse fast Fourier transform, phase compensation, image registration, and image merging. The performance of the proposed algorithm is verified through a simulation and a real experiment with neighboring targets. The results show that the proposed Omega-K algorithm with plane wave approximation can be successfully applied to FIRA systems with bistatic synthetic aperture radar configuration.

Key Words: Forward-Looking Imaging Radar, Omega-K Algorithm, Plane Wave Approximation, Ultra-Wideband, Unmanned Ground Vehicle.

I. Introduction

Synthetic aperture radar (SAR), which can produce high-resolution images regardless of brightness or weather conditions, has been an important and efficient Earth-observing tool that uses microwave frequencies. Although SAR systems have usually been operated from aircraft or orbiting satellite platforms, ground-based SAR (GB-SAR) systems have also been proposed as portable geotechnical instruments [1]. In some applications, vehicle-mounted forward-looking imaging radar (FIRA) using a real aperture has been employed to inspect forward ground surfaces [2–5]. A FIRA system installed on an unmanned ground vehicle (UGV) has also been proposed for visualizing forward areas through vegetation [3]. In many applications, FIRA has usually adopted the multi-input/double-output (MIDO) principle to decrease system complexity, power consumption, weight, and cost.

Most previous research on FIRA has adopted the back-projection (BP) algorithm for image formation [3, 4]. However, the BP algorithm requires additional processing steps to reduce the sidelobes of FIRA images [6] and to increase spatial resolution. In addition, computation time depends on the size of the interested region due to the process that computes pixel-based received signals in the time domain. As alternatives, the range-Doppler method, the Omega-K method, and so on are also available. In FIRA applications, the bistatic configuration is more complicated than the monostatic configuration due to its difficulty and complexity in the formulation of analytic equa-

Manuscript received January 14, 2022 ; Revised April 5, 2022 ; Accepted June 28, 2022. (ID No. 20220114-007J)
Radar/EW Technology Center, Agency for Defense Development, Daejeon, Korea.
*Corresponding Author: Kichul Yoon (e-mail: yoonkc@add.re.kr)

tions and imaging algorithms [7]. In this paper, we describe the Omega-K algorithm in a bistatic configuration that uses plane wave approximation, phase compensation, image registration, and image merging. The next section describes the proposed method in detail, and the effectiveness of the method is verified by a simulation, in the case of point targets, and an experiment, employing a real FIRA introduced in [3].

II. Simplified Bistatic Omega-K Algorithm

1. Forward-Looking Imaging Radar

Sun et al. [3] investigated FIRA, which can detect visually hidden obstacles in vegetation, as a potential asset to support the autonomous navigation of a UGV or an unmanned air vehicle. Fig. 1 shows the schematic geometry of the FIRA system used in the proposed method. The radar system is installed on a commercial vehicle and operates in a frequency range of 3.6 GHz to 5.2 GHz. As shown in Fig. 1, the FIRA system has two transmitting (Tx) antennas located 0.2 m above the ends of the linear array, which is composed of 26 receiving (Rx) antennas. The receiving antennas are horizontally equally spaced at a distance of 0.03 m, and the total length is 0.75 m. The heights of the transmitting antennas and the receiving antenna arrays are 2.1 m and 1.9 m, respectively.

We used commercial horn antennas as transmitting antennas. Since the receiving antennas should be planar, compact in size, and directive with high radiation efficiency to compose a physical array, we used antipodal Vivaldi antennas with a high gain, a relatively wide bandwidth, and a simple structure. The antipodal Vivaldi antenna is advantageous due to its ease of fabrication and small volume. The voltage standing wave ratio is roughly less than 2.1 and the gain greater than 5 dBi over the frequency range of 3.6–5.2 GHz [3].

The transceiver in the FIRA system uses two independent direct digital synthesizers, followed by multipliers, to generate transmitting and local oscillator (LO) signals, respectively. The transmit power is amplified by more than 25 dBm through an amplifier. The received signals pass through low-noise amplifiers, whose noise figure and gain are 2.8 dB and 14 dB, respectively, and are mixed with the LO signal. The signals are then processed after passing through low-pass filters and a 16-bit A/D converter with a sampling frequency of about 400 MHz [3].

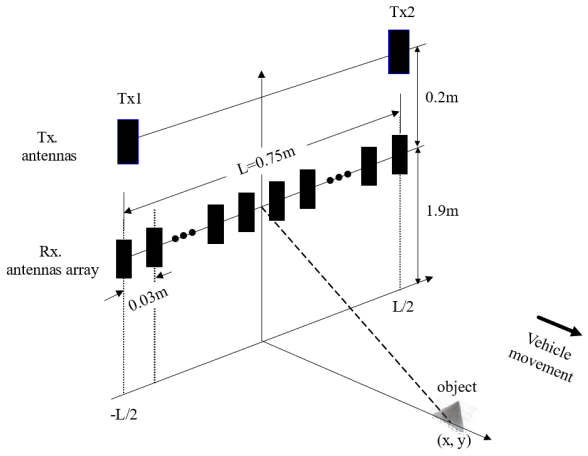

Fig. 1. Schematic geometry of the FIRA system.

2. Bistatic Omega-K Algorithm using Plane Wave Approximation

The target area is composed of an infinite or finite set of stationary targets located at the coordinates (x_n, y_n). The measured signal at the receiving antenna position u and at the fast-time frequency ω is as follows [8]:

$$s_{Txi}(\omega,u)=\sum_n a_n(\omega,x_n,y_n,u_{Txi},u)a(\omega,x_n,y_n,u_{Txi},u)\times exp\left[-jk\sqrt{x_n^2+(y_n-u)^2}\right]\times exp\left[-jk\sqrt{x_n^2+(y_n-u_{Txi})^2}\right], \quad (1)$$

where $a(\cdot)$ is the radar amplitude pattern, $a_n(\cdot)$ the n^{th} target amplitude pattern, and u_{Txi} the position of the i^{th} transmitting antenna.

The Fourier transform of $s_{Txi}(\omega,u)$ with respect to the slow time u, followed by using the stationary phase method, results in the following equation:

$$S_{Txi}(\omega,k_u)=\sum_n A_n(\omega,k_u)A(\omega,k_u)\times exp\left[-j\left(\sqrt{k^2-k_u^2}x_n+k_u y_n\right)\right]\times exp\left[-jk\sqrt{x_n^2+(y_n-u_{Txi})^2}\right]. \quad (2)$$

The second phase term in Eq. (2) originates from the bistatic configuration, and we propose a simplified bistatic Omega-K algorithm using plane wave approximation, as demonstrated in Fig. 2 and the following explanation.

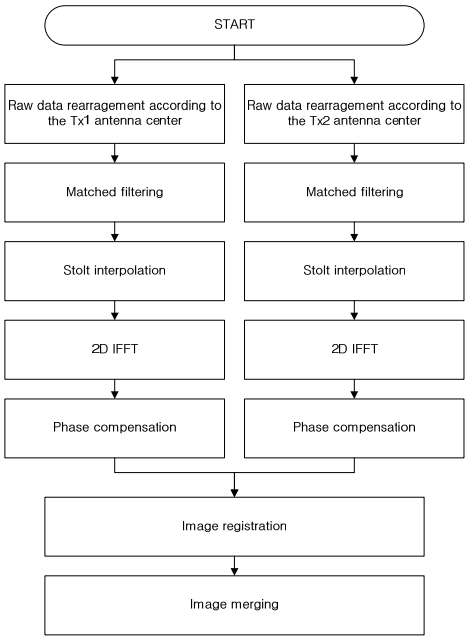

Fig. 2. Flowchart of the proposed method.

First, we assume that each Tx antenna is located at the center of the Rx antenna array, as illustrated in Fig. 3, and that the wave propagates as a plane wave. Consequently, the second phase term in Eq. (2) is simplified to Eq. (3).

$$exp\left[-jk\sqrt{x_n^2+(y_n-u_{Txi})^2}\right] = exp\left[-jk\sqrt{x_n^2+y_n^2}\right] \approx exp(-jkx_n). \quad (3)$$

Substituting Eq. (3) into Eq. (2), we obtain the following equation:

$$S_{Txi}(\omega,k_u) \approx \sum_n A_n(\omega,k_u)A(\omega,k_u) \times exp\left[-j\left\{\left(\sqrt{k^2-k_u^2}+k\right)x_n + k_u y_n\right\}\right] = \sum_n A_n(\omega,k_u)A(\omega,k_u) \times exp\left[-j\left\{k_x(\omega,k_u)x_n + k_y(\omega,k_u)y_n\right\}\right], \quad (4)$$

where

$$k_x(\omega,k_u) = \sqrt{k^2-k_u^2}+k \qquad k_y(\omega,k_u) = k_u \quad (5)$$

Stolt interpolation is performed according to the relationship of Eq. (5). An image can then be obtained by performing a two-dimensional (2D) inverse fast Fourier transform (IFFT).

The error caused by the plane wave approximation along the new coordinate axes centered at each transmitted antenna is compensated for, as shown in Eq. (6).

$$I_{T_{xi}}^{comp}(x_n,y_n) = I_{T_{xi}}(x_n,y_n) \times \exp\left\{-jk\left(\sqrt{x_n^2+y_n^2}-x_n\right)\right\}, \quad (6)$$

where $I_{T_{xi}}(\cdot)$ is the image obtained by 2D IFFT of $S_{T_{xi}}(\omega,k_u)$.

Here, the coordinate axes of the two images obtained through Eq. (6) are not aligned. Therefore, the images must be registered on the original coordinate axis.

Finally, a combined image is created by the coherent summation of pixels from the two images.

III. Simulation and Experiment Results

The performance of the proposed method was analyzed through a simulation and an experiment conducted using the FIRA system developed by the Agency for Defense Development in South Korea [3].

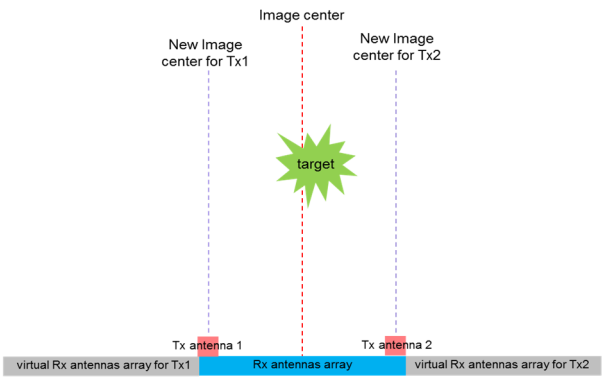

Fig. 3. Concept of plane wave approximation.

1. Simulation Results with Point Targets

In the simulation, the raw data were corrupted by additive white Gaussian noise using MATLAB. Fig. 4 shows the results of the comparison between the images obtained by the BP algorithm and the proposed method. In the first simulation of a point target, the target is located at a range of 10 m with an azimuth of 0 m. As shown in Table 1, the cross-range resolution, or azimuth resolution, and peak side-lobe ratio (PSLR) have similar values for both imaging methods, but the integrated side-lobe ratio (ISLR) of the image obtained by the proposed method is superior to that obtained by the BP method.

In the other simulation, three neighboring point targets are located at $(10\ m, 0\ m)$, $(10\times cos5°m, 10\times sin5°m)$, and $(10\times cos5°m, -10\times sin5°m)$. The proposed algorithm can distinguish the three neighboring targets and achieve image quality comparable to that achieved by the BP method.

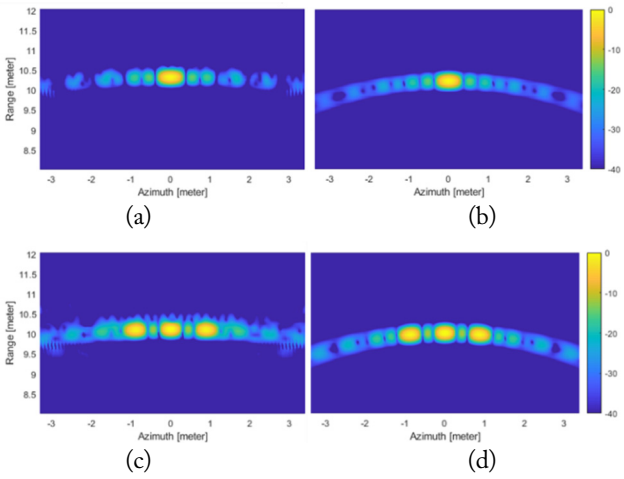

Fig. 4. Simulation results of a point target (a, b) and three neighboring point targets (c, d), obtained from the proposed method (a, c) and the back-projection method (b, d).

Table 1. Quantitative analysis of the image qualities for the FIRA images obtained by the proposed method and the back-projection method

	Back-projection		Proposed	
	Simulation	Experiment	Simulation	Experiment
Azimuth resolution (m)	0.33	0.36	0.34	0.37
PSLR (dB)	14.27	9.89	14.28	10.84
ISLR (dB)	10.79	5.88	9.42	5.62

"Simulation" presented the results of a point target in Fig. 4, and "Experiment" is the results of T1 target in Fig. 5.

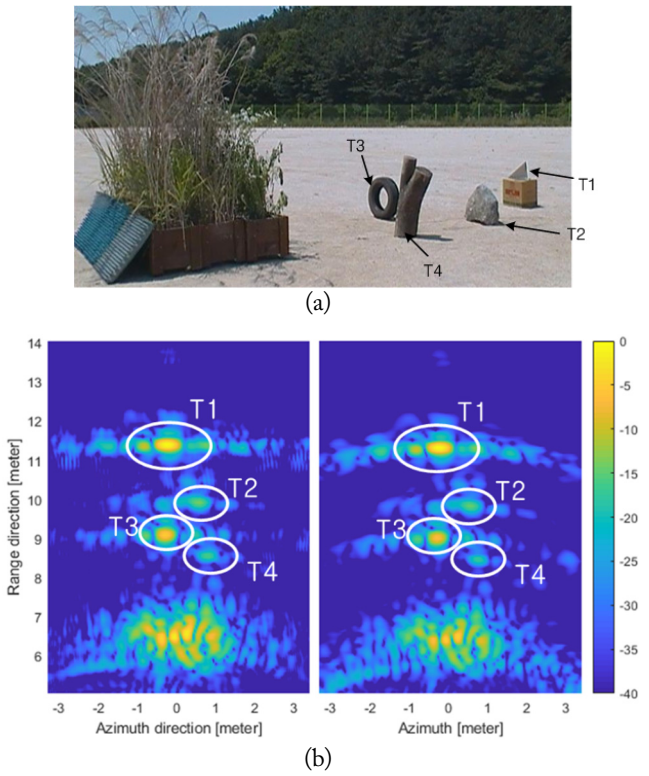

Fig. 5. (a) A photograph of the experimental site and (b) experiment results obtained from the proposed method (left) and the back-projection method (right).

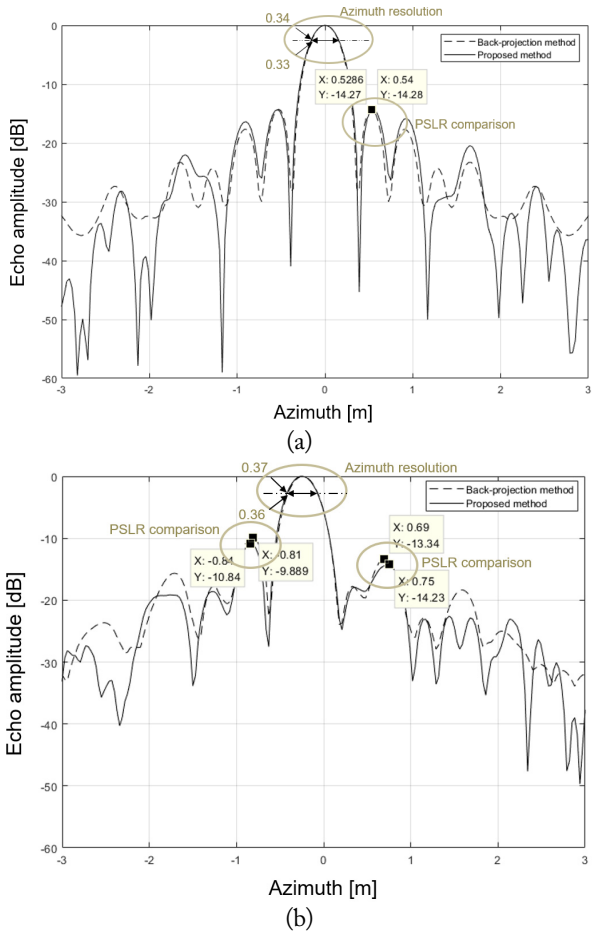

Fig. 6. Azimuth cuts of (a) a point target result in Fig. 4 and (b) T1 target result in Fig. 5 for comparison between the back-projection method and the proposed method.

2. Experimental Results with an Actual FIRA System

The experiments were carried out using the FIRA system described in the earlier section, with a pulse width of 2 ms and a sampling frequency of 400 MHz. A photograph of the measurement site is shown in Fig. 5(a). Four targets (a tree fork, a tire, a rock, and a trihedral corner reflector) on the ground were prepared, and reeds were placed between the targets and the FIRA system, visually hiding the targets from the FIRA system. In Fig. 5(b), the FIRA images by both the proposed method (left) and the BP method (right) show comparable qualities.

More quantitatively, the azimuth resolution, PSLR, and ISLR for the T1 target in Fig. 5(b) are evaluated and summarized in Table 1. The cross-range (azimuth) resolution had similar values for both imaging methods, but the PSLR and ISLR of the image obtained by the proposed method showed better performance than that obtained by the BP method.

For more detailed performance comparison, Fig. 6 presents azimuth cuts of the point target result in Fig. 4 and T1 target result in Fig. 5. The values of the azimuth resolution and PSLR are reconfirmed from the figures in Table 1.

IV. Conclusion

A novel image-formation method that can be used in a FIRA system with an MIDO configuration was proposed. This method is based on a conventional Omega-K algorithm. To resolve the difficulties originating from the bistatic configuration, the following approximation and assumption were used: approximation of spherical wave to plane wave radiating toward the interesting area and assumption that each of the transmitting antennas is located at the center of the receiving antenna array by applying a virtual antenna array. Phase compensation and image registration were then performed to compensate for errors caused by approximation and assumption.

The proposed method was tested through simulations with point targets and experiments using a real FIRA system, and the results were compared with those from the BP method. In terms of image quality, the proposed method and the BP method showed mostly comparable performance, but the PSLR and ISLR of the image obtained by the proposed method was superior to that obtained by the BP method. The proposed method can be applied to bistatic radar imaging systems.

References

[1] B. L. Cho, Y. K. Kong, H. G. Park, and Y. S. Kim, "Auto-

mobile-based SAR/InSAR system for ground experiments," *IEEE Geoscience and Remote Sensing Letters*, vol. 3, no. 3, pp. 401-405, 2006.

[2] S. Yoo, H. Kim, G. Byun, and H. Choo, "Estimation of detection performance for vehicle FMCW radars using EM simulations," *Journal of Electromagnetic Engineering and Science*, vol. 19, no. 1, pp. 13-19, 2019.

[3] S. G. Sun, B. L. Cho, J. S. Lee, G. C. Park, and J. S. Ha, "Ultra-wideband imaging radar to reveal obstacles concealed in vegetation to improve navigation of unmanned ground vehicles," *Journal of Electromagnetic Waves and Applications*, vol. 28, no. 11, pp. 1305-1315, 2014.

[4] L. Nguyen and M. Soumekh, "System trade analysis for an ultra-wideband forward imaging radar," in *Proceedings of SPIE 6230: Unmanned Systems Technology VIII*. Bellingham, WA: International Society for Optics and Photonics, 2006, pp. 13-23.

[5] T. Jin, Q. Song, and B. Lu, "Virtual array imaging radar azimuth resolution analysis," in *Proceedings of IET International Radar Conference*, Guilin, China, 2009.

[6] B. L. Cho, S. G. Sun, and B. G. Lim, "Image enhancement in forward imaging radar using modified apodisation technique," *Electronics Letters*, vol. 49, no. 13, pp. 846-848, 2013.

[7] B. Liu, T. Wang, Q. Wu, and Z. Bao, "Bistatic SAR data focusing using an omega-K algorithm based on method of series reversion," *IEEE Transactions on Geoscience and Remote Sensing*, vol. 47, no. 8, pp. 2899-2912, 2009.

[8] M. Soumekh, *Synthetic Aperture Radar Signal Processing with MATLAB Algorithm*. New York, NY: John Wiley & Sons, 1999.

Byunglae Cho

received a B.S. degree in electronic and electrical engineering from Kyungpook National University in 1999 and M.S. and Ph.D. degrees in electronics and electrical engineering from POSTECH in 2001 and 2005, respectively. In 2005, he was with POSTECH as a postdoctoral researcher for one year. Since 2006, he has worked as a principal researcher at the Agency for Defense Development in Korea. His research interests include SAR, interferometric SAR, forward-looking imaging radar, frequency-modulated continuous wave radar, and active electronically scanned array radar.

Sungwon Hong

received his B.S., M.S., and Ph.D degrees in electronic and electrical engineering from Kyungpook National University, Daegu, South Korea, in 2010, 2012, and 2017, respectively. Since 2017, he has been with the Agency for Defense Development, Daejeon, South Korea. His current research interests include radar system design, signal processing, and performance analysis.

Kichul Yoon

received a B.S. degree in mechanical engineering, Sungkyunkwan University (2011), M.S. degree in mechanical and aerospace engineering, Seoul National University (2013), and Ph.D. degree in mechanical and nuclear engineering, The Pennsylvania State University (2016). In 2016, he joined the Agency for Defense Development in Korea. His research interests include active phased-array radar systems and forward-looking imaging radar systems.